ОБЪЕДИНЕННЫЙ
ИНСТИТУТ
ЯДЕРНЫХ
ИССЛЕДОВАНИЙ
ДУБНА

E4 – 11292

V.G.Soloviev, Ch.Stoyanov, V.V.Voronov

THE INFLUENCE OF THE GIANT DIPOLE RESONANCE ON RADIATIVE STRENGTH FUNCTIONS IN SPHERICAL NUCLEI

1978

E4 – 11292

V.G.Soloviev, Ch.Stoyanov, V.V.Voronov

THE INFLUENCE OF THE GIANT DIPOLE RESONANCE ON RADIATIVE STRENGTH FUNCTIONS IN SPHERICAL NUCLEI

Submitted to "Nuclear Physics"

Соловьев В.Г., Стоянов Ч., Воронов В.В. Е4 - 11292

Влияние гигантского дипольного резонанса на радиационные силовые функции

Рассчитаны E1-силовые функции в широком интервале энергий возбуждения, включая гигантский дипольный резонанс (GDR) для сферических четно-четных ядер в области A = 90-150.

Изучено влияние GDR на радиационные силовые функции. Получено хорошее описание ширины GDR в ^{124}Te, ^{140,142}Ce.

Работа выполнена в Лаборатории теоретической физики ОИЯИ.

Препринт Объединенного института ядерных исследований. Дубна 1978

Soloviev V.G., Stoyanov Ch., Voronov V.V. E4 - 11292

The Influence of the Giant Dipole Resonance on Radiative Strength Functions in Spherical Nuclei

The E1-strength functions for spherical doubly even nuclei are calculated in a wide energy interval including the giant dipole resonance (GDR). A good description of the GDR widths in ^{124}Te, ^{140}Ce and ^{142}Ce is obtained. The calculated values of the radiative strength functions near the neutron binding energy B_n are in good agreement with the experimental data. The influence of GDR on the radiative strength functions and on the total photoabsorption cross sections is studied. It is shown that in single-closed-shell nuclei the E1-strength functions near B_n are slightly influenced by GDR. The values of strength functions are determined by the fragmentation of one-phonon states lying near B_n. For nuclei far from the closed shells, the influence of GDR on the radiative strength functions increases, and, for example, in ^{136}Ba, ^{144}Nd and ^{146}Nd it becomes essential. The dipole photoabsorption $\sigma_{\gamma t}$ cross sections as functions of the excitation energy are calculated. The existence of substructures, but not their energy location, is reliably predicted by the theory. The available experimental data confirm the existence of substructures in the energy dependence of $\sigma_{\gamma t}$. It is shown that the Lorentzian extrapolation of the GDR tail proved to be rough for the description of $\sigma_{\gamma t}$ near B_n.

Preprint of the Joint Institute for Nuclear Research. Dubna 1978

1. INTRODUCTION

In recent years we are occupied with the calculation of a few-quasiparticle components of the nuclear wave functions at low, intermediate and high excitation energies within the quasiparticle-phonon nuclear model [1-3]. The characteristics of the neutron and giant multipole resonances in many nuclei have been studied on the basis of strength functions without finding the roots of the corresponding secular equations. The fragmentation of the one-quasiparticle states in deformed nuclei has been studied and the strength functions of the one-nucleon transfer reactions and the neutron strength functions have been calculated in ref. [4]. The neutron strength functions for the tin and tellurium isotopes have been calculated in ref. [5]. The giant multipole resonances in spherical nuclei have been studied in ref. [6]. In that paper the fragmentation of the one-phonon states due to the quasiparticle-phonon interaction was investigated. The mathematical apparatus developed in ref. [6] can be used for calculating the partial radiative strength functions [7].

The radiative strength functions and the influence of the giant dipole resonance (GDR) on them have been analyzed in a number of reviews [8-13]. To study the radiative strength functions the Brink-Axel treatment is widely used, according to which the dependence of the radiative widths on energy is determined by the Lorentz distribution of the GDR tail. The analysis of the radiative strength

functions[10] has shown that the Lorentz extrapolation of GDR overestimates the values of the E1-strength functions in the low-energy region for nuclei near closed shells. Up to now the influence of GDR on the partial strength functions has been studied only within the phenomenological methods. In the framework of the quasiparticle-phonon nuclear model one can calculate the radiative E1-strength functions and the total photoexcitation cross-sections in a wide interval of excitation energies and study the influence of GDR.

The aim of this paper is to calculate the radiative strength functions $b(E\lambda, E)$ in a wide energy interval including the GDR region, and to study the influence of GDR on them. The necessary formulae and the discussion of the numerical details are given in Sec. 2. The results of calculation of GDR in doubly even spherical nuclei are discussed in Sec. 3. Section 4 contains the investigation of the fragmentation of one-phonon states, and the results of calculation of the radiative strength functions near the neutron binding energy B_n. The influence of GDR on the E1-strength functions and on the total photoabsorption cross sections and the behaviour of the total photoabsorption cross section as a function of the excitation energy are discussed in Sec. 5. Section 6 contains the conclusions.

2. FORMULAE AND NUMERICAL DETAILS

To calculate the E1-strength functions for the transitions from the ground states of doubly even spherical nuclei, we use a version of the quasiparticle-phonon model developed in ref.[6]. The model Hamiltonian includes the average field for neutrons and protons, superconducting pairing interactions and multipole-multipole and spin-multipole-spin-multipole forces. Both the isoscalar and isovector forces are used. An important role is played by the quasiparticle-phonon interaction. The explicit form of the model

Hamiltonian, provided that the secular equations in the RPA are satisfied, is given in ref.[6].

We take into account the coupling between the one-phonon and two-phonon components. Thus, the wave function of an excited state is

$$\Psi_\nu(JM) = \{\sum_i R_\nu(Ji) Q^+_{JMi} + \sum_{\substack{\lambda_1 i_1 \\ \lambda_2 i_2}} P^{\lambda_1 i_1}_{\lambda_2 i_2} [Q^+_{\lambda_1 \mu_1 i_1} Q^+_{\lambda_2 \mu_2 i_2}]_{JM}\}|0\rangle_{ph}, \quad (1)$$

where $|0\rangle_{ph}$ is the phonon vacuum and, at the same time, the ground state of a doubly even nucleus, $Q^+_{\lambda\mu i}$ is the phonon creation operator, and ν is the number of an excited state. The quantity $R^2_\nu(Ji)$ determines the contribution of the one-phonon state to the normalization condition of the wave function (1). The secular equation defining the energies $\eta_{J\nu}$ of the states and the quantities $R^2_\nu(Ji)$ are given in ref.[6].

The fragmentation (i.e., the distribution of strength) of the one-phonon states over many nuclear levels is calculated in the framework of the given model. Using the fragmentation of the one-phonon states, one can easily calculate the reduced $E\lambda$-transition probabilities and the total photoexcitation cross sections from the ground states of doubly even nuclei. Neglecting the terms $\approx a^+a$ in the $E\lambda$-transition operator, the $B(E\lambda)$-values are expressed through $R_\nu(\lambda i)$ as follows:

$$B(E\lambda; O^+_{g.s.} \to \lambda\nu) = \sum_i R_\nu(\lambda i) \sqrt{B(E\lambda; O^+_{g.s.} \to \lambda i)_{RPA}}, \quad (2)$$

where $B(E\lambda; O^+_{g.s.} \to \lambda i)_{RPA}$ is the reduced $E\lambda$-transition probability calculated within the RPA.

To calculated the radiative strength functions we apply the method which was used earlier in refs.[4-7,14]. By this method the average values are calculated without solving the secular equations. The strength function for the $E\lambda$-transitions from the ground

state of a doubly even nucleus to the levels in the energy interval $\eta - \frac{1}{2}\Delta$, $\eta + \frac{1}{2}\Delta$ is

$$b(E\lambda;\eta) = \frac{1}{2\pi} \sum_{\nu} \frac{\Delta}{(\eta - \eta_{\lambda\nu})^2 + \frac{1}{4}\Delta^2} B(E\lambda; 0^+_{g.s.} \to \lambda\nu), \qquad (3)$$

where the summation of ν runs over the states in the interval $\eta - \frac{1}{2}\Delta$, $\eta + \frac{1}{2}\Delta$. The explicit form of the strength function (3) is given in ref./6/. The method of strength functions is an important part of the quasiparticle-phonon nuclear model. This is due to the fact that in this model only few quasiparticle components of the wave function rather than the whole wave function are described correctly. The strength functions are determined by the fragmentation of few quasiparticle components. In our case the radiative strength functions are determined by the fragmentation of the one-phonon components. Instead of diagonalizing the matrix of higher order and finding all the components (which are very numerous) of the wave function for each state, we calculate the imaginary parts of the determinants at different excitation energies η with step Δ.

The parameter Δ may be considered to be a way of representation of the results of calculation. If Δ is very small, the strength function is a series of narrow peaks of the Breit-Wigner form. With increasing Δ the peaks become broader, their amplitudes decrease and the fine structure gradually disappears. Thus, by varying Δ, we can reproduce the strength function in a much detail as we wish. The value of Δ can be taken to be equal to the experimental energy resolution.

It should be noted that by introducing the parameter Δ one can take into account the influence of many-phonon components of the wave functions which are not explicitly taken into account. Thus, the problem is to calculate the values of Δ. Now we write the expressions for the radiative strength functions and the dipole photoabsorption cross section. The

results of calculation for them will be given in what follows. We use the following definition of the radiative strength functions:

$$\langle k(E\lambda)\rangle = \sum_{\nu\in\Delta} \Gamma_{\gamma_0}(E\lambda,\eta_\nu)/(E^{2\lambda+1} A^{2/3\lambda} \Delta)(\mathrm{MeV}^{-(2\lambda+1)}), \qquad (4)$$

$$\sum_{\nu\in\Delta} \Gamma_{\gamma_0}(E1,\eta_\nu) = 0.35 \int_{E-\frac{1}{2}\Delta}^{E+\frac{1}{2}\Delta} \eta^3 b(E1,\eta) d\eta\,(\mathrm{eV}), \qquad (5)$$

where

$$\sum_{\nu\in\Delta} \Gamma_{\gamma_0}(E2,\eta_\nu) = 1.61\cdot 10^{-7} \int_{E-\frac{1}{2}\Delta}^{E+\frac{1}{2}\Delta} \eta^5 b(E2,\eta)\, d\eta\ (\mathrm{eV}) \qquad (6)$$

and E is the energy. The average cross section of the dipole photoabsorption is

$$\sigma_{\gamma t}(E) = 4.025\, E/\Delta \int_{E-\frac{1}{2}\Delta}^{E+\frac{1}{2}\Delta} b(E1,\eta) d\eta\ (\mathrm{mb}). \qquad (7)$$

Note, that the contribution of the M1 and E2-cross sections of photoabsorptions is not large in comparison with the cross-section (7).

The details of numerical calculations are given in ref. /6/ We use the Saxon-Woods potential with the parameters given in Table 1 in ref./6/. To perform additional calculations in the zone A=141, Z=59, the parameters are taken the same as in the zone A=127, Z=53 in Table 1 of ref./6/. The only exception is the parameter V_0: for which V_0 = 46.5 MeV for the neutron and V_0 = 58.1 MeV for the proton system. The values of the pairing constants are fixed from the experimental data on pairing energies/15/. The constants of the quadrupole and octupole forces are chosen so as to reproduce the experimental data on the 2^+_1 and 3^-_1 level when calculating with the wave function (1). The isovector constants κ^{λ}_{1} are expres-

sed in terms of the isoscalar constants κ^{λ}_{0} as follows: $\kappa^{2}_{1}=-1.5\kappa^{2}_{0}$, $\kappa^{3}_{1}=-4.5\kappa^{3}_{0}$. The constants of the multipole-multipole interactions with $3<\lambda<8$ are somewhat smaller than the estimates of ref./14/. Therefore the structure of the first states was close to that of two-quasiparticle ones. When calculating the characteristics of the dipole excitations, the spurious states have been excluded by the method of ref./16/.

In comparison with paper/6/ we have described more correctly the spin-multipole-spin-multipole interaction. Following ref./17/ the constants of this interaction are calculated by the following formula:

$$\kappa^{(S\lambda)}_{\sigma 0}=\kappa^{(S\lambda)}_{\sigma 1}=-\frac{100\pi}{A<r^{2S-2}>}. \qquad (8)$$

Such a choice of the constants allowed one to describe correctly the experimental data on the M1 -resonances/18/. The one-phonon space is described in detail in ref./3/. In our calculations in the wave function (1) we take up to 14 one-phonon and approximately 1000 two-phonon components.

In our approach we treat phonons as bosons, neglecting their fermion structure, and therefore to a certain extent we violate the Pauli principle when constructing the two-phonon components. The problem of elimination of the terms violating the Pauli principle is studied in many papers, for instance, in ref./19/. It is shown in paper/3/ that within the quasiparticle-phonon model, one can carry out calculations with "ideal" bosons. Then, the Pauli principle is strictly fulfilled in each approach. The use of the "ideal" bosons results mainly in the shift of the two-phonon pole energies. This effect to a great extent can be compensated by the renormalization constants which are fitted to experimental energies of the first λ^{π}_{1} levels. Besides, as in paper/6/ we introduce the following limitations to the wave function (1). One of the phonons in its two-phonon part is to be collective. As a result, the function (1) completely loses the components consisting of two noncollective phonons which may just violate the Pauli principle. Therefore, the inaccuracies due to the violation of the Pauli principle do not exceed other inaccuracies of our calculation.

3. THE GIANT DIPOLE RESONANCE

We start with the results of calculation for the giant dipole resonance in spherical nuclei, and then we go over to the discussion of the radiative strength functions and the influence of GDR on them. The results of calculation of GDR in ^{90}Zr, , ^{120}Sn and ^{124}Te are given in ref./6/. In our paper a more correct description of the spin-multipole phonons does not change strongly the results for ^{90}Zr and ^{120}Sn, though the contribution of individual components has changed. The results of calculation of GDR for ^{124}Te have changed considerably. The total E1 -photoabsorption cross section for ^{124}Te calculated with Δ = 0.4 MeV is given in Fig. 1. This Figure also shows the experimental data /20/ on the total photoneutron cross sections. It is known that a part corresponding to the E1 -transitions gives a 99% contribution to the total photoabsorption cross section. The Figure shows that a qualitative description of the shape of GDR is obtained. In our calculation the central peak is higher and the fine structure is exhibited more explicitly in comparison with the experiment. This is perhaps due to the fact that in our wave function (1) many-phonon components are not taken into account. A better

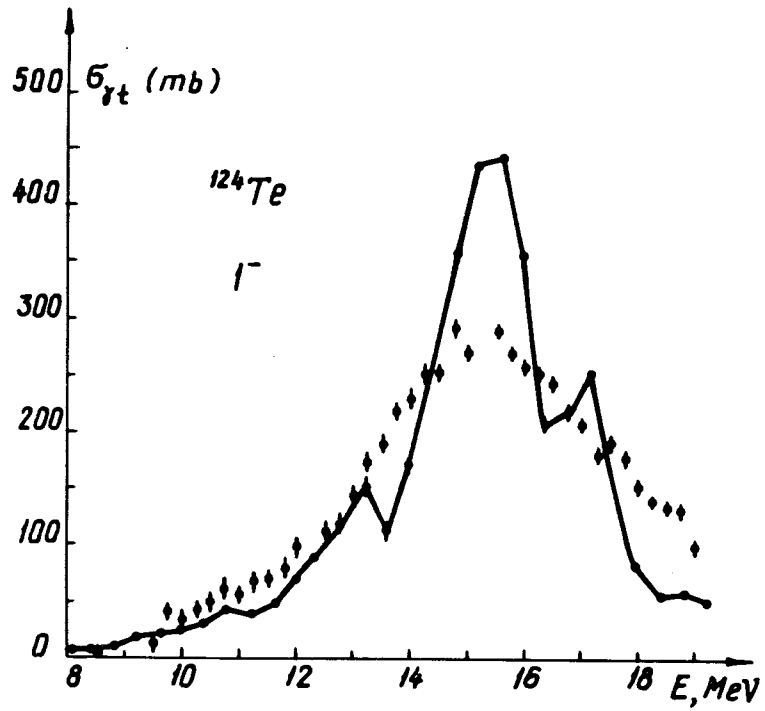

Fig. 1. Photoabsorption cross section $\sigma_{\gamma t}$ for ^{124}Te. Points by a solid line denote the calculation with Δ = 0.4 MeV. Points are the experimental data from ref./20/.

description of the shape of GDR for ^{124}Te in this paper in comparison with ref./6/ is mainly due to a more correct description of the spin-multipole phonons. As it was indicated in ref./21/ the widths of GDR are determined from its coupling with the low-lying collective states. Our calculation testifies to the fact that for the description of the shape of giant multipole resonances one should take into account a large number of weakly collectivized phonons besides strongly collectivized low-lying phonons /21/.

The total dipole photoabsorption cross sections for ^{140}Ce and ^{142}Ce were measured in ref./20/. A specific feature of these nuclei is that the GDR width in ^{142}Ce is considerably larger than in ^{140}Ce. Our results and the experimental data for ^{140}Ce and ^{142}Ce are given in Figs. 2 and 3, respectively. As it is seen from these Figures our calculations demonstrate correctly the lowering of the peak $\sigma_{\gamma t}$ and the increase of the GDR width when passing from ^{142}Ce to ^{140}Ce. The broadening of GDR in ^{142}Ce as compared to ^{140}Ce is naturally explained within our model. The role of anharmonic effects, which mainly determine the value of the GDR width, increase when passing from single-closed-shell to nonmagic nuclei.

Paper/20/ contains different integrated cross sections obtained from the experimental data and defined by the expressions

$$\sigma_0 = \int_{B_n}^{E_M} \sigma_{\gamma t}(E)dE \quad (MeV \cdot b), \tag{9}$$

$$\sigma_{-1} = \int_{B_n}^{E_M} E^{-1} \sigma_{\gamma t}(E)dE \quad (mb), \tag{10}$$

$$\sigma_{-2} = \int_{B_n}^{E_M} E^{-2} \sigma_{\gamma t}(E)dE \quad (mb \cdot MeV^{-1}), \tag{11}$$

where E_M is the upper integration limit. Since in our calculation, the upper limit for ^{124}Te E_M = 19 MeV, we have recalculated the corresponding experimental data following Fig. 9 of ref./20/. An analogous procedure has been carried out for the ^{140}Ce and ^{142}Ce nuclei.

It should be noted that the quasiparticle-phonon model correctly describes the change of the GDR characteristics (the values of $\sigma_{\gamma t}$ maximum, width and integral cross sections) when passing from one nucleus to another. The results of calculation and the experimental data on the integrated cross sections are given in Table 1. It is seen from this Table that the cross sections calculated are very close to the corresponding experimental values.

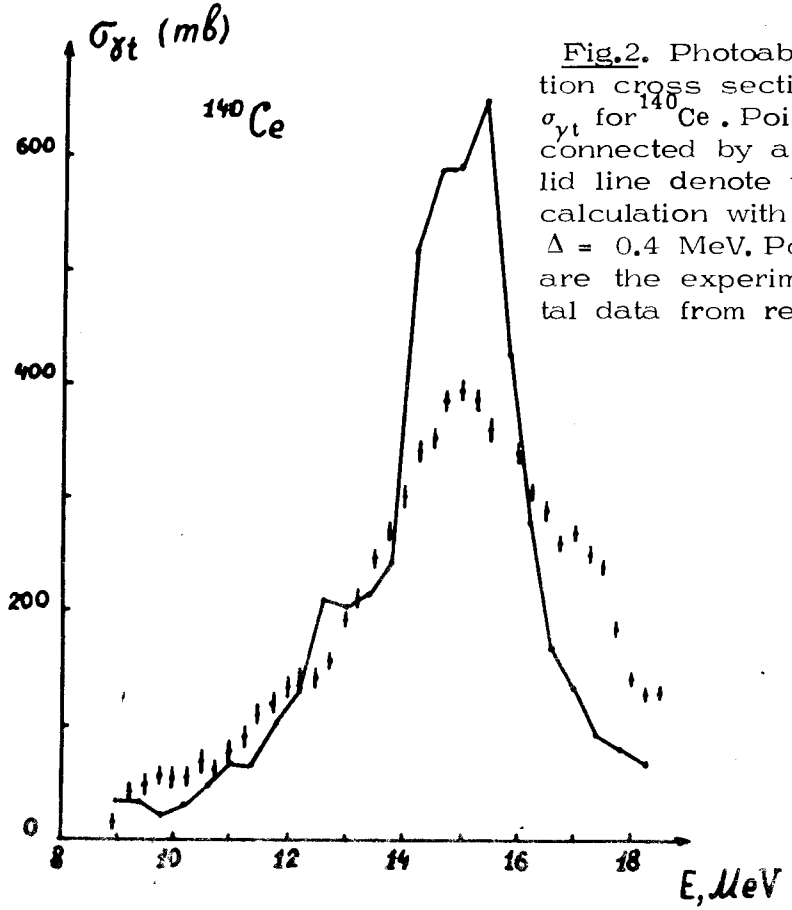

Fig.2. Photoabsorption cross section $\sigma_{\gamma t}$ for ^{140}Ce. Points connected by a solid line denote the calculation with Δ = 0.4 MeV. Points are the experimental data from ref. /20/

Table 1

Integrated photoneutron cross sections

Nucleus	^{124}Te		^{140}Ce		^{142}Ce	
	E_M=19.0 MeV		E_M=18.5 MeV		E_M=17.4 MeV	
	Experim.	Calc.	Experim.	Calc.	Experiment.	Calc.
σ_0 (B.MeV)	1.46	1.52	1.77	1.90	1.89	1.96
σ_1 (mb)	98.7	102.9	123	137	131.8	142
σ_{-2} (mb.MeV^{-1})	6.6	7.0	8.8	9.8	10.2	10.5

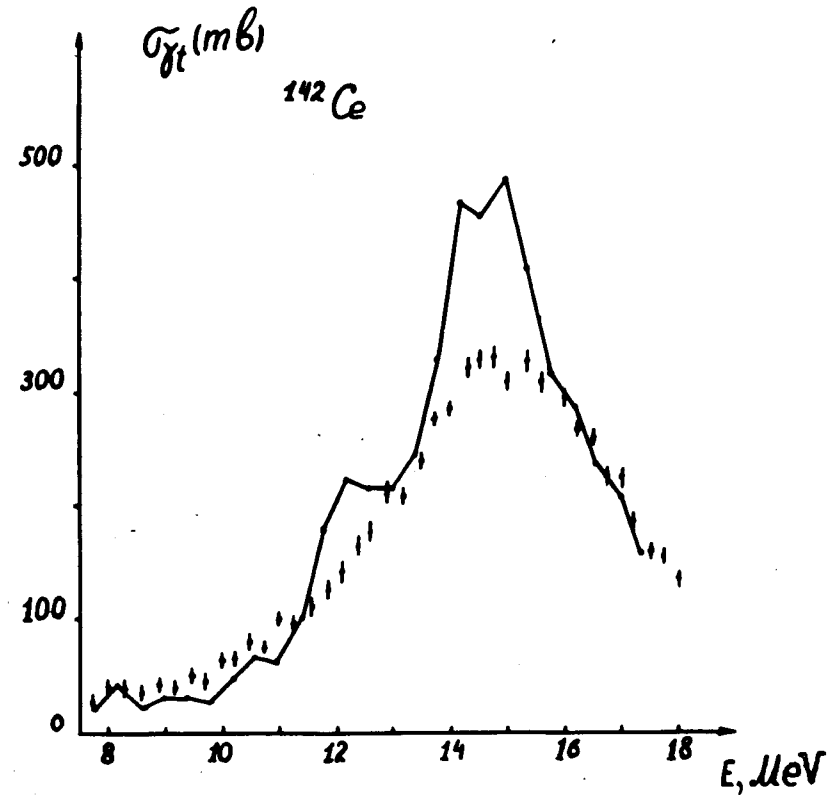

Fig. 3. Photoabsorption cross section $\sigma_{\gamma t}$ for ^{142}Ce. Points connected by a solid line denote the calculation with Δ = 0.4 MeV. Points are the experimental data from ref. /20/.

4. RADIATIVE STRENGTH FUNCTIONS

The fragmentation of one-phonon states over two-phonon ones can easily be calculated in this version of the quasiparticle-phonon model with the wave function (1). Having the $R_\nu(\lambda i)$ values one can calculate the reduced $E\lambda$ -transition probabilities from the ground states of doubly even nuclei by formula

(2). To calculate the $E\lambda$ -transitions from the one-phonon states, one should know the fragmentation of the two-phonon ones. The fragmentation of the two-phonon states can be calculated by including additional three-phonon components into the wave function (1) and by solving the system of equations which can easily be derived from equations of ref. /22/.

We study the radiative strength functions for the E1 -transitions in doubly even spherical nuclei. We are dealing with the fragmentation of the one-phonon 1^- states and the behaviour of B(E1) -values. An important information about the dipole strength distribution can be extracted from the calculation of the energy weighted sum rule (EWSR). Calculating EWSR in the energy interval ΔE, we use the following formula;

$$S_{\Delta E} = \sum_{\nu \in \Delta E} \eta_\nu B(E1\uparrow, \eta_\nu) = \int_{\Delta E} Eb(E1\uparrow, E)dE \, (e^2 fm^2 \, MeV). \quad (12)$$

The RPA calculations show that the first 1^- states in spherical nuclei lie at energies (7-9) MeV, though experimentally they are observed at an energy of 6 MeV and lower (see refs. /23-25/). These low-lying 1^- states are due to the fragmentation of the one-phonon states. The lowering of the 1^- states is demonstrated by the example of ^{140}Ce and ^{136}Ba.

In the RPA, in the region (7-9) MeV in ^{140}Ce there are 8 solutions, the lowest 1^- state being of an energy of 7.3 MeV. These solutions give a 0.78% contribution to the model independent EWSR. Due to the quasiparticle-phonon interaction several 1^- states appear in the region (5.7-7.1) MeV, which give a 0.18% contribution to the EWSR. The total contribution to the EWSR from the states lying below 9 MeV increases up to 1.1%. It should be noted that ^{140}Ce is a single-closed-shell nucleus, and therefore the one-phonon states in it are fragmented not so strongly as in nonmagic ones.

The RPA calculations show that for ^{136}Ba in the region (7-9) MeV there are 7 solutions, the lowest state

being of an energy of 7.67 MeV. These solutions give a 2.03% contribution to the model independent EWSR. The quasiparticle-phonon interaction produces several 1^- states in the region (4.3-7.6) MeV. The first state is of an energy of 4.3 MeV. These states give a 0.44% contribution to the model independent EWSR. The one-phonon states forming GDR are taken into account in these calculations. The total contribution of the states lying below 9 MeV to the model independent EWSR increases up to 2.54%.

Based on our calculations one can explain the existence of the low-lying 1^- states in spherical nuclei the wave functions of which have distinct one-phonon components.

The E1 and E2 radiative strength functions for transitions from the gound states to the levels near B_n are calculated within the quasiparticle-phonon nuclei. Table 2 shows the results of calculation for those nuclei for which there are the corresponding experimental data. The $\langle k(E\lambda)\rangle$-values determined by eq. (4) are calculated with $\Delta = 0.2$ MeV. The calculated values of $\langle k(E\lambda)\rangle$ differ from the corresponding experimental data not more than by a factor of 2. Note, that we have obtained a better agreement between the theory and experiment in comparison with the calculations of ref. /7/. This is due to a better description of the spin-multipole phonons which enter into the two-phonon part of the wave function (1).

It should be noted that such a good agreement of the theory with experiment is not trivial, since the calculations have no free parameters. Indeed, the results of calculation depend on the value of Δ. However, for the Fe, Ba and Ce isotopes the $\langle k(E\lambda)\rangle$ values change not more than by a factor of 2 upon changing Δ from 0.5 to 2 MeV. The accuracy of our calculation does not pretend to give a correct description of small local maxima of b(E1,E) as functions of the excitation energy. Therefore it is senseless to calculate with $\Delta < 0.1$ MeV. It is also unreasonable to use the values of Δ larger than (0.5-1.0) MeV since

Table 2

Radiative strength functions

Nucleus	E MeV	Eλ	⟨K(Eλ)⟩ × 10⁹ MeV^-(2λ+1) Experim.	Reference	Calcul.
^{56}Fe	11.2	E1	1.7	26	1.7
^{90}Zr	8.7	E1	3.25		2.2
	10.0	E1	3.25	24	5.1
	11.3	E1	6.24		7.2
	11.9	E1	7.1		9.6
Sn	6.4	E1	5.02		3.2
	7.0	E1	4.2	24	4.6
	8.6	E1	8.35		9.5
^{136}Ba	9.1	E2	1.02×10^{-4}	27	1.2×10^{-4}
^{138}Ba	8.6	E1	4.0	28	3.9
^{140}Ce	9.08	E1	2.2	29	2.1

at large values of Δ the specific features of the function b(Eλ,E) are smoothed.

5. THE ANALYSIS OF THE RADIATIVE STRENGTH FUNCTION AND PHOTOABSORPTION CROSS SECTIONS

To analyze the E1-strength functions the Brink-Axel treatment is often used, according to which the

dependence of the dipole photoabsorption cross sections on the energy is defined by the Lorentz distribution of the GDR tail. In this case the photoabsorption cross section has the following form:

$$\sigma_{\gamma t}(E) = \sigma_0 \frac{\Gamma_0^2 E^2}{(E^2 - E_0^2)^2 + E^2\Gamma_0^2}, \qquad (13)$$

where E_0 is the energy and Γ_0 is the width of GDR. It is assumed that the Lorentz form fits well the energy dependence in nuclei far from the closed shells. However, the Lorentz extrapolation of GDR overestimates the values of the E1-strength functions near B_n for the nuclei near the closed shells. Indeed, for ^{138}Ba the experimental value [28] $\langle k(E1)\rangle = 4\cdot10^{-9}$ whereas according to eq. (13) $\langle k(E1)\rangle = 9\cdot10^{-9}$. In ^{140}Ce the experimental value [29] $\langle k(E1)\rangle = 2.2\cdot10^{-9}$ whereas the Lorentz extrapolation gives $9.8\cdot10^{-9}$.

Note, that eq. (13) is a particular case of eq. (7). The cross section (13) can be obtained from eq. (7) under the following assumptions: a) GDR is formed by one collective one-phonon state; b) all the matrix elements entering into the secular equations are equal to each other; c) the density of two-phonon poles is proportional to $E^{1/2}$. These assumptions are not valid in spherical nuclei. It is shown in ref. [6] that GDR is formed by several collective one-phonon states. The matrix elements differ from each other strongly.

Let us study the influence of GDR on the behaviour of the radiative strength functions $b(E1^{\uparrow}, E)$ in an energy interval of about (6-10) MeV. First we calculate $b(E1^{\uparrow}, E)$ with the wave function (1) the one-phonon part of which has only the RPA solutions lying in an interval of about (6-10) MeV. In this case the function $b(E1^{\uparrow}, E)$ is determined by the fragmentation of the one-phonon states lying within the above energy interval. The results of these calculations for ^{124}Te, ^{144}Nd and ^{146}Nd are denoted in Figs. 4, 5 and 6 by the dashed lines.

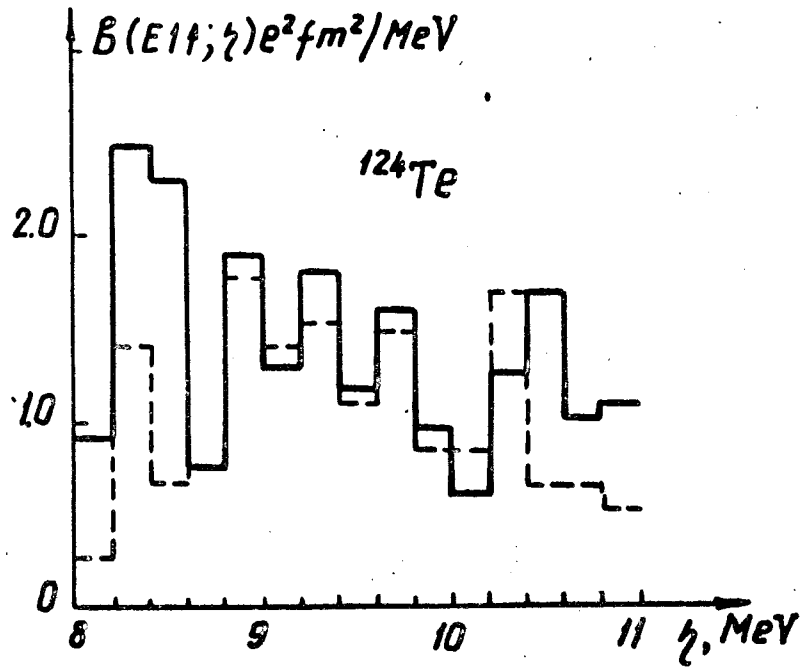

Fig. 4. Histogram of the strength function $b(E1\uparrow,\eta)$ in ^{124}Te. Calculation taking into account GDR (solid line). Calculation without taking into account GDR (dashed line).

Now we calculate $b(E1\uparrow,E)$ in the same energy intervals but with the wave function (1) which also consists of the one-phonon states forming GDR. A difference in the behaviour of the function $b(E1\uparrow,E)$ calculated with and without GDR determines the influence of the GDR on the E1-radiative strength functions. The results of calculations which take into account the phonons forming GDR are denoted in Figs. 4-6 by the continuous lines. It is seen from these figures that the GDR influences strongly the E1 -strength functions of these nuclei. The influence

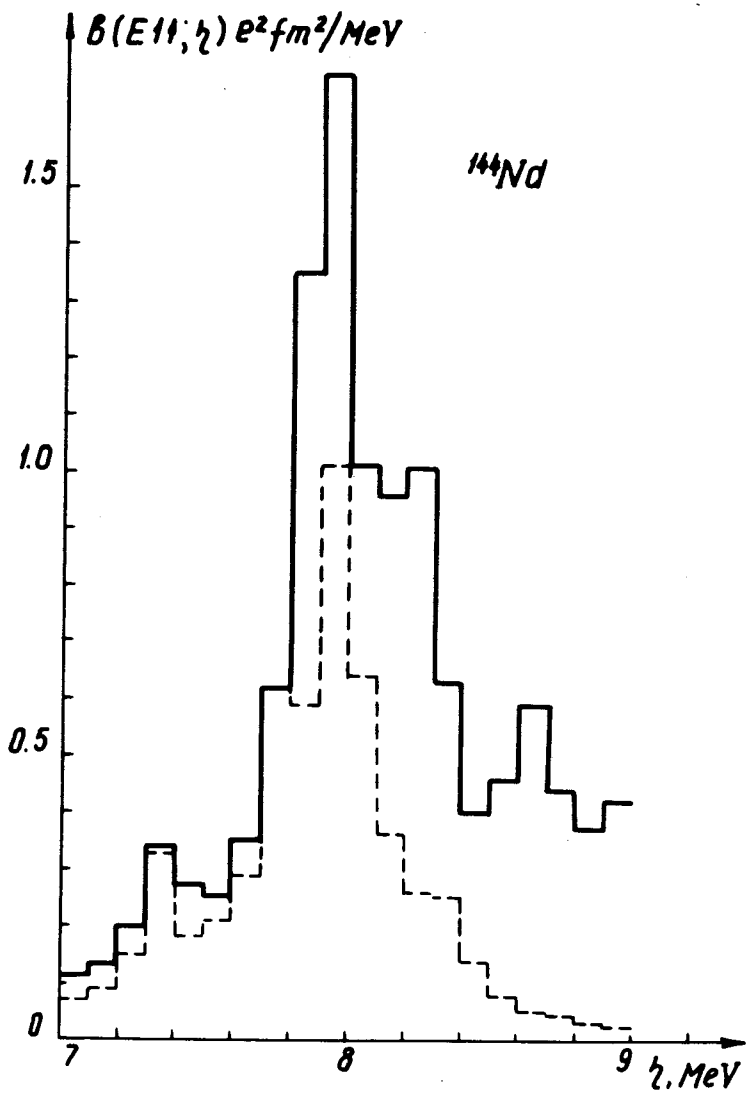

Fig. 5. Histogram of the strength function $b(E1\uparrow,\eta)$ in ^{144}Nd. Calculation taking into account GDR (solid line). Calculation without taking into account GDR (dashed line).

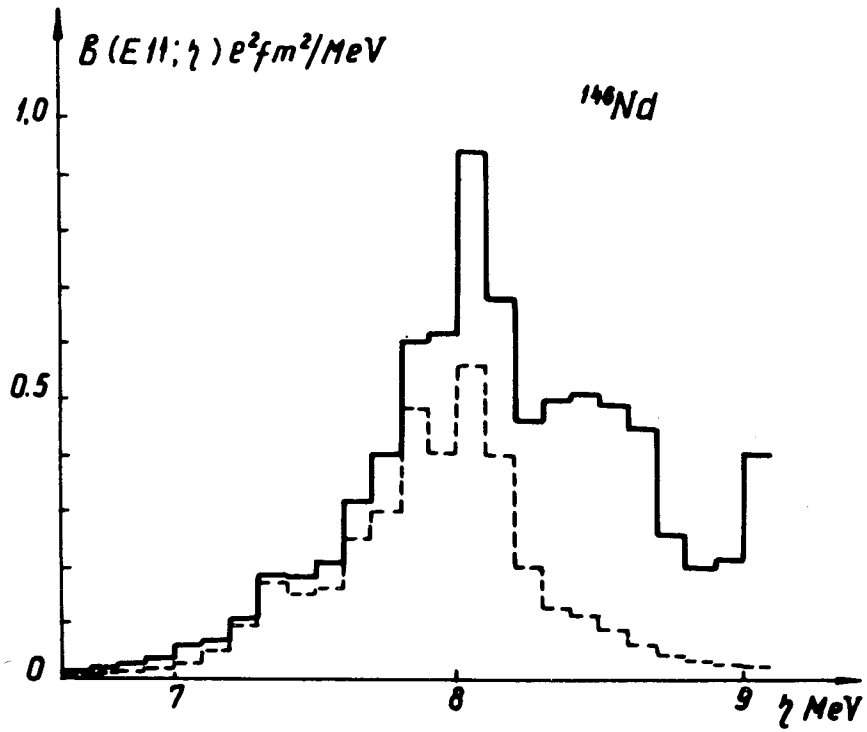

Fig. 6. Histogram of the strength function $b(E1\uparrow,\eta)$ in ^{146}Nd. Calculation taking into account GDR (solid line). Calculation without taking into account GDR (dashed line).

of GDR on $b(E1\uparrow,E)$ increases with increasing excitation energy.

Figures 4-6 show the nonmonotonic behaviour of $b(E1\uparrow,E)$ as a function of the excitation energy. These substructures are due to the neighbouring one-phonon states and to the influence of the GDR strength.

We have studied the influence of GDR on the radiative strength functions for many nuclei from Zr to Nd by calculating $S_{\Delta E}$ (see eq. (12)) in the energy

interval ΔE with and without GDR. The results of calculations are given in Table 3. The functions $S_{\Delta E}(0)$ are calculated with the one-phonon states lying in the interval ΔE. The functions $S_{\Delta E}$ (GDR) are calculated taking into account additional phonons which form GDR. It is seen from Table 3 that in ^{90}Zr and ^{118}Sn the influence of GDR on $b(E1\uparrow,E)$ is small. In ^{90}Zr function $S_{\Delta E}$ increases considerably in the interval (8-10) MeV if the one-phonon states lying above 10 MeV and below GDR are taken into account. The influence of GDR is also very small in other tin isotopes. Representing the function $b(E1\uparrow,E)$ as histograms of the type of Fig. 4 for the tin isotopes, one can see that the lines for the cases when GDR is taken into account and without it practically coincide. The influence of GDR on the radiative strength functions is also not too large in the single-closed-shell nuclei ^{138}Ba, ^{140}Ce and ^{142}Nd.

Based on the above calculations we may conclude that the influence of GDR on the functions $b(E1\uparrow,E)$ in the region of B_n is small in single-closed-shell nuclei. In these nuclei the function $b(E1\uparrow,E)$ to a great extent is determined by the fragmentation of one-phonon states lying near B_n. One can see from Table 3 that the influence of GDR on $b(E1\uparrow,E)$ is stronger for nonmagic nuclei than for single-closed-shell nuclei. So, in ^{144}Nd and ^{146}Nd the function $S_{\Delta E}$(GDR) is larger than $S_{\Delta E}(0)$ more than by a factor of two. The influence of GDR does not mean a general increase of the function $b(E1\uparrow,E)$. GDR makes some redistribution of dipole strength over the energy interval. As a result $b(E1\uparrow,E)$ as a function of the excitation energy E demonstrates irregularities.

It should be noted that calculating the functions $b(E1\uparrow,E)$ in the energy interval ΔE, one should take into account the RPA-solutions lying in this interval ΔE even if they give a small contribution to $b(E1\uparrow,E)$ and $S_{\Delta E}$. These one-phonon terms in the wave function (1) should be also taken into account

Table 3

Influence of GDR on functions $S_{\Delta E}$

Nucleus	Number of one-phonon comp.in (1)	Energy interval for one-phonon comp.(MeV)	Energy interval ΔE of summation for $S_{\Delta E}$ (MeV)	$S_{\Delta E}$ fm²MeV	$\frac{S_{\Delta E}^{(GDR)}}{S_{\Delta E}^{(0)}}$
^{90}Zn	9	8-13	8-13	9.43	1.19
	10	8-13,16		11.2	
^{118}Sn	4	6-10	6-10	1.83	1.09
	14	6-16		1.99	
^{124}Te	6	8-11	8-11	2.95	1.3
	14	8-16		3.82	
^{136}Ba	8	8.3-10.3	8.3-10.3	8.6	1.67
	14	8.3-15		14.3	
^{138}Ba	6	7-9	7-9	10.4	1.5
	14	8.3-15		15.5	
^{140}Ce	5	8-10	8-10	5.03	1.33
	14	8-15		6.68	
^{142}Ce	4	8-9.2	4.0-9.2	9.34	1.74
	14	8-14.9		16.25	
^{142}Nd	6	8.4-11.3	8.8-11.3	15.2	1.52
	14	8.4-15.8		23.1	
^{144}Nd	3	7-9	7-9	4.12	2.4
	14	7-15.9		9.97	
^{146}Nd	4	7.5-9	6.5-9	3.0	2.2
	14	7.5-15		6.6	

when $b(E1\uparrow,E)$ is strongly influenced by GDR. This is due to the fact that the RPA-solutions affect the behaviour of $b(E1\uparrow,E)$ in the energy region of their location. In some cases the weak one-phonon states prevent the penetration of the GDR strength into the energy location region of these solutions.

Now we calculate the total photoexcitation cross sections $\sigma_{\gamma t}$ and compare the results with the corresponding experimental data and with the Lorentzian curve. The cross sections $\sigma_{\gamma t}$ for ^{90}Zr measured in ref./24/ and calculated by us are given in Fig. 7. It is seen from this figure that the general form of cross sections is of the Lorentz type. There are some irregularities in the energy dependence of the experimental and calculated cross sections. The calculated cross sections up to an energy of 10 MeV are slightly influenced by GDR, whereas at high energies the role of GDR increases. GDR slightly affects the dipole photoabsorption cross sections in the tin isotopes calculated in ref./30/.

The dipole photoabsorption cross sections are calculated for ^{138}Ba. They are compared with the cross sections measured on the natural barium in ref./25/. The calculated cross section $\sigma_{\gamma t}$ has a bump at an energy of 8.2 MeV. This bump is larger than that observed experimentally at an energy of 7.8 MeV. The experimental cross section $\sigma_{\gamma t}$ has a substructure at an energy of 6.7 MeV, whereas in our calculations it is much less. The calculated cross sections $\sigma_{\gamma t}$ have substructures, and the energy dependence of $\sigma_{\gamma t}$ differs strongly from the Lorentzian curve.

The results of calculation for the cross section $\sigma_{\gamma t}$ in ^{140}Ce and the experimental data for the natural cerium measured in ref./25/ are denoted in Fig. 8. Since the natural cerium contains 89% of ^{140}Ce, one can compare in detail the theory with experiment. The experimental cross section $\sigma_{\gamma t}$ has a maximum at an energy of 7.8 MeV, and the calculated cross section has a higher maximum at an

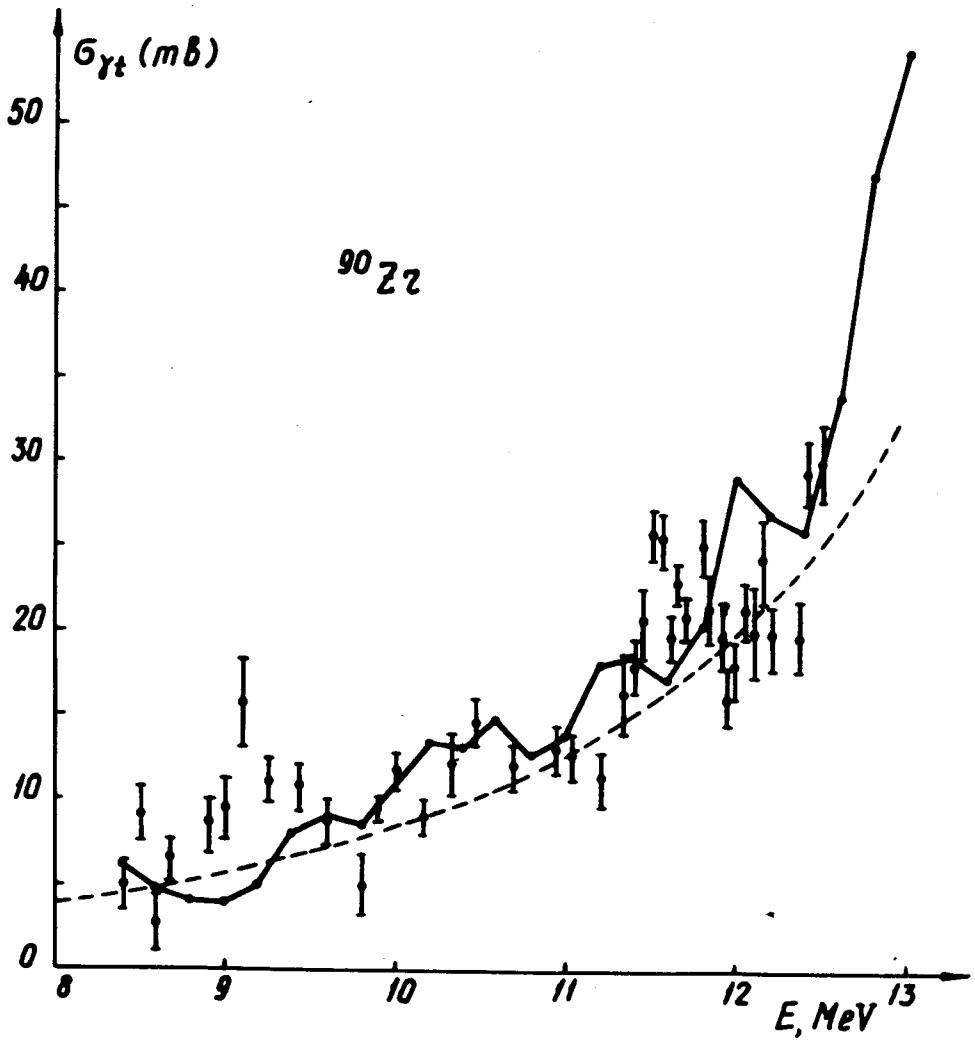

Fig. 7. Dipole photoabsorption cross sections in ^{90}Zr. The experimental data are obtained in ref./24/. Calculations (solid line) are carried out with $\Delta = 0.2$MeV. The Lorentzian (dashed line) is calculated in ref./24/.

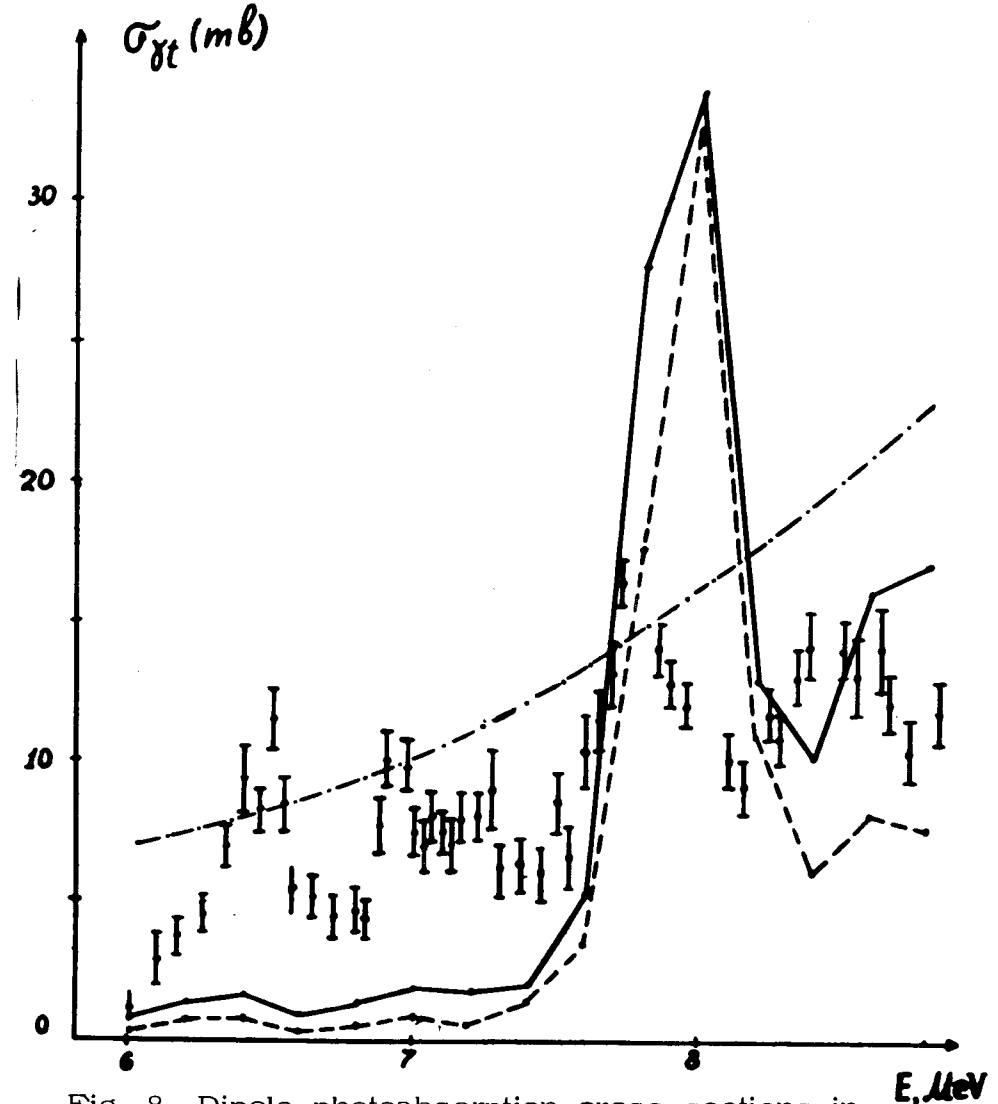

Fig. 8. Dipole photoabsorption cross sections in ^{140}Ce. The experimental data are obtained for the natural cerium/25/. Calculations with taking into account GDR are denoted by the solid line, without taking into account GDR by the dashed line. The Lorentzian (dot-dash line) is calculated in ref./25/ with $E_\sigma = 15$MeV, $\Gamma = 4.35$MeV and $\sigma = 360$ mb.

energy of 8 MeV. In our calculation the fragmentation of one-phonon states is much weaker in single-closed-shell nuclei than in nuclei far from the closed shells. This is the reason for the appearance of such a large peak at an energy of 8 MeV. The increase of the cross section at an energy higher than 8.2 MeV is correctly demonstrated in our calculations. The calculated cross sections are smaller than the experimental ones at an energy less than 7.5 MeV. Perhaps the peaks observed at the energies 6.5 and 7 MeV are due to the impurities of other cerium isotopes. Figure 8 shows also the results for the case when the phonons forming GDR have not been taken into account. It is seen from Fig. 8 that the cross section $\sigma_{\gamma t}$ is slightly influences by GDR. However, the role of GDR increases at an excitation energy higher than 8 MeV.

The energy dependence of the total dipole photoabsorption cross section differs strongly from the Lorentzian curve. Thus, we may conclude that the representation of the photoabsorption cross section near B_n as the Lorentzian is rather rough. One can clearly see the substructures in the total dipole photoabsorption cross section. Our calculations show that such substructures should exist. However, the calculations are not sufficiently accurate to predict the exact location of them.

6. CONCLUSION

Within the quasiparticle-phonon nuclear model one can calculate the radiative strength functions and the total photoabsorption cross sections in a wide energy region including GDR. The widths and shape of GDR are described correctly what is demonstrated by the example of the ^{124}Te, ^{140}Ce and ^{142}Ce nuclei.

It should be noted that within the quasiparticle-phonon nuclear model, one can take into account a large number of multipole and spin-multipole pho-

nons with λ from 1 to 8. A large number of weakly collectivized phonons strongly affects the strength functions at intermediate and high excitation energies. It was shown in ref.[4] that to calculate the fragmentation of one-quasiparticle states in deformed nuclei, a large phonon space should be taken into account. A direct calculation of the strength functions without finding the roots of the relevant secular equations allows one to use a large phonon space and to perform calculations for several nuclei in a wide energy interval.

The quasiparticle-phonon interaction causes the fragmentation of one-phonon states. Due to the fragmentation there appear rather low 1^- states the wave functions of which have noticeable one-phonon components. Thus, we can explain rather low 1^- states in doubly even spherical nuclei observed experimentally.

Based on the study of GDR and its influence on the E1-radiative strength functions $b(E1\uparrow,E)$ we can make the following conclusions. In single-closed-shell nuclei the function $b(E1\uparrow,E)$ is slightly influenced by the GDR tail at energies near B_n. The function $b(E1\uparrow,E)$ is mainly determined by the fragmentation of one-phonon states near B_n. The influence of GDR on $b(E1\uparrow,E)$ is stronger for nonmagic nuclei than for single-closed-shell nuclei. In such nuclei as ^{136}Ba, ^{144}Nd and ^{146}Nd it is essential. The influence of GDR on $b(E1\uparrow,E)$increases with increasing excitation energy. The Lorentzian extrapolation of the GDR tail proved to be rather rough for the description of the total dipole photoabsorption cross sections in the region of B_n.

Our calculations have shown that there should exist the substructures in the energy dependence of the dipole photoabsorption cross sections. The available experimental data on the total photoabsorption cross sections indicate the existence of some substructures. Within the given version of the quasiparticle-phonon model one can predict the substruc-

tures rather than their exact energy location. Perhaps the substructures in nuclei with A from 90 to 140 and the pigmy resonances in nuclei with A = 195–205 are caused by the same reasons.

The authors are grateful to A.I.Vdovin for useful discussions and help.

REFERENCES

1. Soloviev V.G. Izv.Akad.Nauk SSSR (ser. fiz.), 1971, 35, p.666; Theor. Mat. Fiz., 1974, 24, p.137.
2. Soloviev V.G., Malov L.A. Nucl.Phys., 1972, A196, p.433.
3. Soloviev V.G. JINR, E4-11012, Dubna, 1977.
4. Malov L.A., Soloviev V.G. Nucl.Phys., 1976, A270, p.87; Yad. Fiz., 1977, 26, p.729.
5. Dambasuren D. et al. J.Phys. G: Nucl.Phys., 1976, 2, p. 25.
6. Soloviev V.G., Stoyanov Ch., Vdovin A.I. Nucl. Phys., 1977, A228, p.376.
7. Voronov V.V., Soloviev V.G., Stoyanov Ch. Pis'ma JETP, 1977, 25, p.459.
7. Lane A.M. Statistical Properties of Nuclei, ed. J.B.Garg (Plenum Press, New York, 1972), p.271.
9. Chrien R.E. Nuclear Structure Study with Neutrons, ed. J.Szücs (Plenum Press, New York, 1974) p.101; Neutron Capture Gamma-Ray Spectroscopy (Reactor Centrum Nederland, Petten, the Netherlands) p.247.
10. Bartholomew G.A. et al. Advances in Nuclear Physics, 1973, 7, p.229.
11. Bird J.R. et al. Proc. Int. Conf. on Interactions of Neutrons with Nuclei, ed. E.Sheldon (Univ. of Lowell, Lowell, Mass., 1976, v.1, p.77). Allen B.J., Del Musgrove A.R. Advances in Nuclear Physics, to be published.
12. Bergvist I. Proc. Int. Conf. in Interactions of Neutrons with Nuclei, ed. E.Sheldon (Univ. of Lowell, Lowell, Mass., 1976, v.1, p.99).

13. Urin M.G. Part. and Nucl., 1977, 8, p.817; Martsynkevich B.A., Rudak E.A. Nucl.Phys., 1976, A262, p.261.
14. Bohr A., Mottelson B. Nuclear Structure, vols. 1 and 2 (W.A.Benjamin Inc. New York, Amsterdam, 1969 and 1974).
15. Soloviev V.G. Theory of Complex Nuclei (Nauka, M., 1971; Pergamon Press, Oxford, 1976).
16. Peterson D.F., Veje C.J. Phys.Lett., 1967, 24B, p.449.
17. Castel B., Hamamoto I. Phys.Lett., 1976, 65B, p.27.
18. Vdovin A.I., Stoyanov Ch., Yudin I.P. JINR, P4-11081, Dubna, 1977.
19. Belyaev S.T., Zelevinsky V.G. Nucl.Phys., 1962, 39, p.582. Marumori T., Yamanura M., Tokunage A. Prog.Theor.Phys., 1964, 31, p.1009; Dönau F., Janssen D., Frauendorf S., Jolos R.V. Nucl.Phys., 1976, A262, p.291.
20. Lepretre A. et al. Nucl.Phys., 1976, A258, p.350.
21. Balashov V.V. Nucl.Phys., 1963, 40, p.93. Le Torneux J. Phys.Lett., 1964, 13, p.325; Danos M., Greiner W. Phys.Lett., 1964, 8, p.113.
22. Kyrchev G., Soloviev V.G. Theor.Mat. Fiz., 1975, 22, p.244.
23. Wolf A., Moreh R., Shakal O. Nucl.Phys., 1974, A227, p.373.
24. Axel P., Min K.K., Sutton D.C. Phys.Rev., 1970, C2, p.689.
25. Nuclear Physics Research with Electrons from MUSL-2 and MUSL-3. (Dep. of Physics, University of Illinois at Urbana-Champaign, 1977).
26. Balgman R.J., Bowman C.D., Berman B.L. Phys. Rev., 1971, C3, p.672; Abramov A.I., Kitaev V.Ya., Yutkin M.G. Yad.Fiz., 1974, 20, p.438.
27. Chrien R.E. et al. Phys.Rev., 1974, C9, p.1622.
28. Holt R.J., Jackson H.E. Phys.Rev., 1975, C12, p.56.

29. Laszewski R.M., Holt R.J., Jackson H.E. Phys. Rev., 1976, C13, p.2257.
30. Voronov V.V., Soloviev V.G. Proc. of IV Conf. on Neutron Physics, Kiev, 1977, v. 1, p.41; JINR, E4-10506, Dubna, 1977.

Received by Publishing Department
on January 30,1978.